Observation of incoherent picosecond magnetisation dynamics in micron sized $Ni_{81}Fe_{19}$ elements by time resolved scanning Kerr effect microscopy

A. Barman, V.V. Kruglyak, R.J. Hicken, A. Kundrotaite and M. Rahman

Abstract: We have studied small amplitude magnetisation precession in a square $Ni_{81}Fe_{19}$ element by time resolved scanning Kerr effect microscopy. A single precessional mode was observed with a 1 μm diameter probe spot placed at the centre of the element. Using a coherent rotation model, the presence of a four-fold anisotropy of about 30 Oe was deduced. Time resolved images show that the dynamic magnetisation is initially nonuniform at the edges of the element, with the nonuniformity then extending towards the centre. The dynamic magnetisation is uniform at the centre of the element over the measurement time, justifying the use of the coherent rotation model in the analysis of the precession frequency.

1 Introduction

Precessional magnetisation dynamics will play an increasingly important role in the operation of magnetic random access memory (MRAM), magnetic recording head technology and high-speed spin electronics. The optical pump-probe technique is ideal for studying high frequency dynamics in lithographically defined elements. The time resolved scanning Kerr effect microscope (TRSKEM) has been used to perform stroboscopic magnetic imaging [1, 2] of magnetisation reversal [3, 4]. However, small amplitude oscillations are also of interest; first, they provide additional insight into the mechanisms governing the reversal process; and secondly, they may be used to characterise properties such as magnetic anisotropy and interlayer exchange coupling [5]. The optical technique can provide images of finite wavelength excitations with excellent temporal resolution, yet so far only a few attempts have been made to exploit this application of ultrafast microscopy [3, 6, 7, 8]. In this paper we describe the apparatus required to perform stroboscopic imaging of magnetisation dynamics and demonstrate the capabilities of the technique with results from a 10 μm square $Ni_{81}Fe_{19}$ element.

The TRSKEM combines the optical pump-probe technique with scanning laser microscopy. A laser beam from a Ti-sapphire laser (wavelength, 790 nm; repetition rate, 82 MHz; pulse width, 120 fs) is divided into an intense pump and weak probe beam. The ratio of the probe beam power to the pump beam power used in the present experiment is 1 : 20. The pump beam is used to generate an ultra-short magnetic field pulse that is in turn used to excite the sample. The probe beam is used to detect the sample response by means of a magneto-optical Kerr rotation measurement. The device used to generate the magnetic field pulse consisted of an interdigitated photoconductive switch of Au on intrinsic GaAs with 10 μm track width and separation, and a transmission line of Au on GaAs with 30 μm track width and separation [9]. A bias voltage of 20 V was applied to one end of the transmission line while the photoconductive switch was connected to the other end. Two 47 Ω surface mount resistors were connected between the end of the transmission line and the voltage terminals to absorb the current pulse. The pulse profile was also monitored, by measuring the voltage across one of the surface mount resistors with a 500 MHz oscilloscope. The sample was fabricated on a glass substrate and was placed face down on the transmission line tracks so that it could be probed through the substrate. A plane polarised probe beam was focused on to the sample using a microscope objective (NA = 0.65), which was corrected for use with a glass cover slip of 0.17 mm thickness. A drop of immersion oil was placed between the sample and the transmission line. This gave a good back-reflected intensity image while holding the sample firmly in place on the transmission line. The full width at half-maximum of the focused spot was estimated to be 0.75 μm from the Abbé criterion. The pump beam was chopped and the polarisation state of the back-reflected probe beam was analysed by means of an optical bridge detector and a lock-in amplifier. In the present study we measured only the polar Kerr rotation of the reflected probe beam. The sample mount was attached to a piezoelectric scanning stage so that the sample could be scanned with respect to the fixed probe beam. This also causes the focused pump beam to move relative to the photoconductive switch. However, the focused spot and the area of the interdigitated region are sufficiently large that no change in the current pulse is observed during the scan. A rotating electromagnet was used to vary the strength and orientation of the applied static field **H** in the plane of the sample.

The 500 MHz bandwidth of the oscilloscope used to monitor the pulsed field was insufficient to resolve the true pulse shape. The pulse profile was instead determined by an electro-optic sampling [10] technique in which a $LiNbO_3$ crystal of 0.5 mm thickness was placed on top of the

IEE Proceedings online no. 20030868

doi:10.1049/ip-smt:20030868

Paper first received 11th February 2003 and in revised form 28th July 2003

A. Barman, V.V. Kruglyak and R.J. Hicken are with the School of Physics, University of Exeter, Exeter EX4 4QL, UK

A. Kundrotaite and M. Rahman are with the Department of Physics and Astronomy, University of Glasgow, Glasgow G12 8QQ, UK

transmission line. The stray electric field from the transmission line induces a transient birefringence that modifies the polarisation of an initially plane polarised probe beam. Figure 1 shows the electro-optic signal when the probe beam was focused through the $LiNbO_3$ crystal, at normal incidence, at points both on and between the tracks of the transmission line. The 10–90 rise time of the pulse was found to be about 35 ps. Secondary peaks, due to reflections of the current pulse on the transmission line, were also apparent at longer time scales. The peak amplitude of the pulsed field was estimated to be about 27 Oe based upon the voltage measured across the terminating resistor.

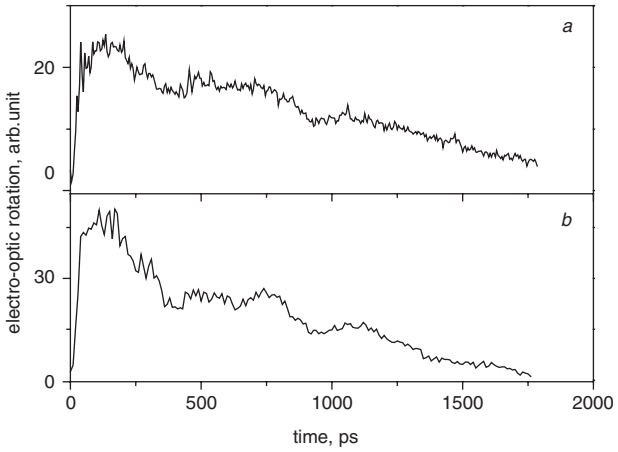

Fig. 1 *Transient optical rotations from the $LiNbO_3$ crystal*
a With the laser focused through the crystal to a point between the transmission line tracks
b With the laser focused to a point in the centre of a transmission line track

The sample was fabricated by electron-beam lithography and sputtering. A bilayer of PMMA resist was first spun onto a glass coverslip of thickness 0.17 mm and the pattern was written by electron beam lithography. A 150 nm thick layer of $Ni_{81}Fe_{19}$ was sputtered (base pressure 2×10^{-7} Torr) on top of the developed resist, followed by a 20 nm thick capping layer of Al_2O_3. A magnetic field of 150 Oe was applied in the plane of the substrate during growth to set the inplane uniaxial anisotropy axis of the sample parallel to one edge of the square. Finally, the unexposed resist was lifted off and an array of square dots of 10 μm side and 60 μm edge-to-edge separation was obtained.

The optical pump-probe measurements were performed using the geometry shown in Fig. 2*a*. The dots were placed on the transmission line in such a way that some lay between the tracks of the transmission line where they experienced an out-of-plane pulsed magnetic field. Two measurement schemes were used. First, the field strength H was varied with **H** applied parallel to an edge and a diagonal as shown in Fig. 2*b*. Secondly, the orientation of **H** (ϕ_H) was varied from 0 to 360° in steps of 10°. In each case the probe beam was positioned at the centre of the element. Figure 2*c* shows typical transient Kerr rotation scans obtained with **H** applied parallel to an edge and a diagonal. Fast Fourier transforms of this data reveal the presence of a single mode in each case. The field dependence of the mode frequency is plotted in Fig. 3*a* for different static field orientations. In Fig. 3*b* the dependence of mode frequency upon ϕ_H is plotted when $H = 254$ Oe. There is a clear four-fold symmetry, the frequency being a maximum (minimum)

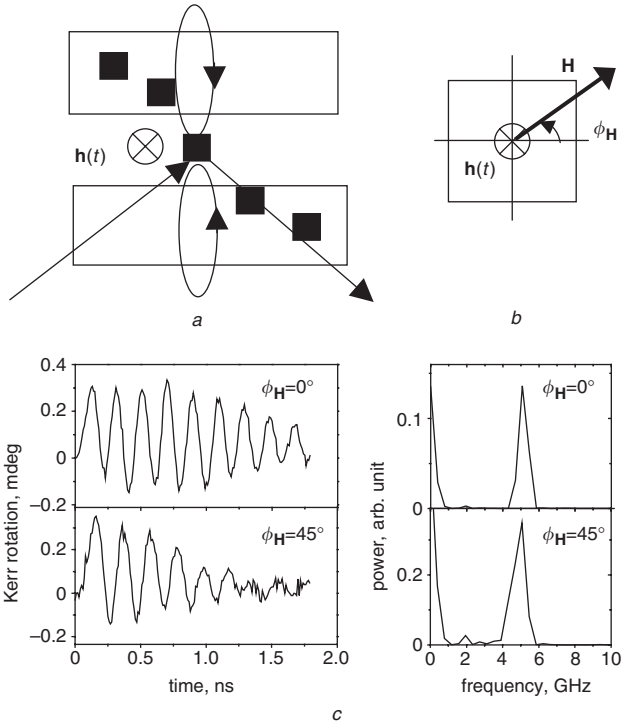

Fig. 2 *Transient Kerr rotation scans obtained with a static field of 254 Oe*
a Sample layout and measurement geometry
b Orientation of **H** and **h**
c Scans obtained with **H** applied parallel to an edge ($\phi_H = 0°$) and a diagonal ($\phi_H = 45°$) of the element, and corresponding FFTs

when **H** is parallel to an edge (diagonal), suggesting that the edges are the easy axis directions. Brillouin light scattering data has shown similar results [11] for a close-packed array of elements.

The variation of the frequency has been modelled by solving the Landau–Lifshitz equation in the limit of a small amplitude uniform precession. We assume that the energy density associated with the magnetic anisotropy has the form $-K_2(\mathbf{u}.\mathbf{k})^2 + K_4(u_x^4 + u_y^4)$ where K_2 and K_4 are, respectively, the uniaxial and four-fold anisotropy constants, **u** is a unit vector parallel to the magnetisation vector, **k** is a unit vector parallel to the uniaxial easy axis, and the x- and y-axes lie in the plane of the element parallel to its edges. The precession frequency is given by

$$f = \frac{\gamma}{2\pi}\left\{\begin{array}{l}[H\cos\phi + \frac{2K_2}{M}\cos 2(\phi-\phi_2) \\ \quad - \frac{4K_4}{M}\cos 4(\phi-\phi_4)] \\ [H\cos\phi + \frac{2K_2}{M}\cos^2(\phi-\phi_2) \\ \quad - \frac{K_4}{M}(3+\cos 4(\phi-\phi_4)) + 4\pi M]\end{array}\right\}^{\frac{1}{2}} \quad (1)$$

where, $\gamma = g\mu_B/\hbar$. Here M is the magnetisation and g is the gyromagnetic ratio, while ϕ, ϕ_2 and ϕ_4 are the angles that the magnetisation, the uniaxial easy axis and the x-axis describe with **H**. The frequencies were simulated by assuming quasi-alignment of the magnetisation with the static field (see Fig. 3). The strong four-fold symmetry of Fig. 3*b* suggests that any additional uniaxial anisotropy term is relatively small. Values of $4\pi M = 10.8$ kOe, $g = 2.1$, $2K_2/M = 2$ Oe and $4K_4/M = -33$ Oe were used in the simulations of the FMR frequencies.

The precession frequency seems to be well described by the coherent rotation model. However, to investigate the

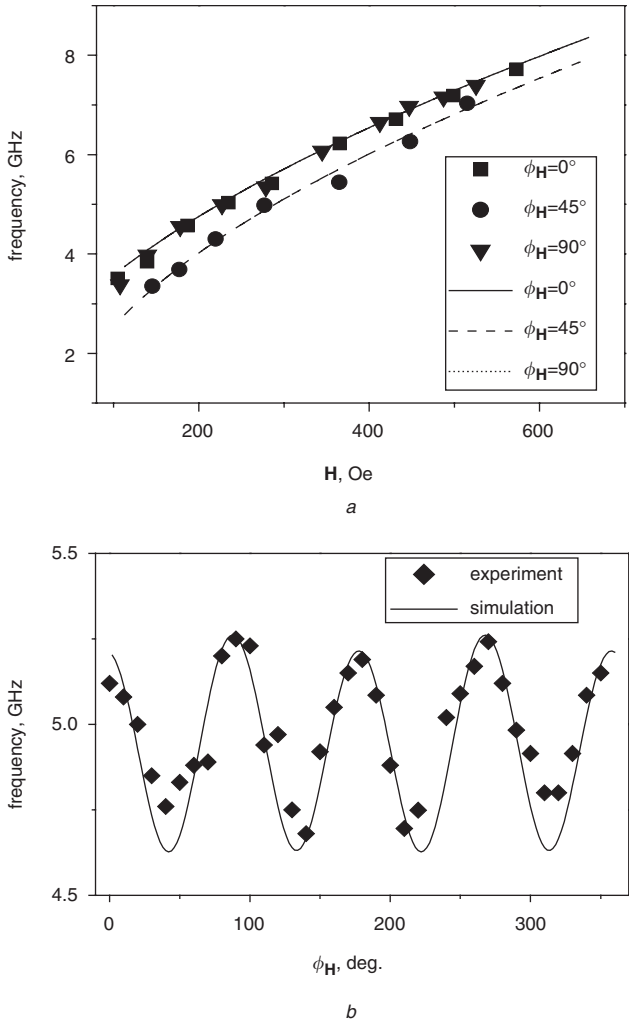

Fig. 3 *Measured (symbols) and simulated (curves) precession frequencies*
a For various values of $\phi_{\mathbf{H}}$ as H is varied
b For $H = 254$ Oe as $\phi_{\mathbf{H}}$ is varied, revealing a four-fold symmetry

uniformity of the dynamic magnetisation we acquired a series of dynamic images at different times after excitation with the pulsed magnetic field. The pixel size in each scan was 0.5 μm and the grey scale represents the instantaneous value of the out-of-plane component of the precessing magnetisation. Fig. 4*a* shows the orientation of **H** and **h** for the measurement of dynamic images. Fig. 4*b* shows the optical image of the sample while in Fig. 4*c* dynamic magnetic images are shown at various delay times. The dynamic image at 120 ps shows that the magnetisation begins to precess almost uniformly over the entire area of the sample. Nonuniformity is apparent after 350 ps at the edges of the element that lie perpendicular to the static field. The two dark stripes correspond to regions where the magnetisation precesses with a different phase to the rest of the sample. The nonuniformity gradually extends towards the centre of the element in the images at 690, 1130, 1330 and 1480 ps, although the central region, where the probe spot is positioned, remains reasonably uniform. Nonuniform precession in circular dots has been reported and explained in terms of a nonuniform internal and external pulsed field [3]. In our experiment the pulsed field was believed to be uniform to within 10% over the area of the sample, and we believe that the nonuniform dynamic response results from the nonuniform static and dynamic dipolar fields that occur in an element that is not ellipsoidal in shape.

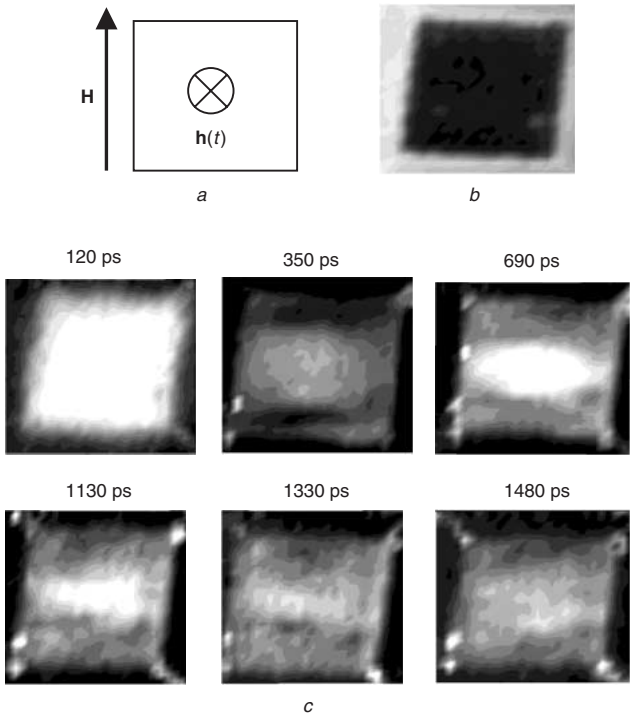

Fig. 4 *Dynamic magnetic imaging measurements*
a Experimental geometry
b Optical intensity image
c Dynamic magnetic images for various delay times, $H = 254$ Oe

2 Conclusions

We have studied small amplitude precession in a square $Ni_{81}Fe_{19}$ element by time resolved scanning Kerr effect microscopy. The precession at the centre of the element was modelled by means of a coherent rotation model. A four-fold symmetry was observed in the dependence of the precession frequency upon the static field orientation, corresponding to a four-fold anisotropy field of about 30 Oe. We have acquired time-resolved images in order to investigate the uniformity of the magnetisation dynamics within the element. We observed that nonuniformity first appears near the edges of the element that lie perpendicular to the static field, and gradually moves towards the centre of the element. However, the central region remains uniform for a sufficiently long time that the use of the coherent rotation model in the analysis of the precession frequency appears to be justified. Micromagnetic simulations are now required to better understand the spatial variation of the dynamic magnetisation.

3 Acknowledgments

The authors gratefully acknowledge the financial support of the UK Engineering and Physical Sciences Research Council.

4 References

1 Hiebert, W.K., Stankiewicz, A., and Freeman, M.R.: 'Direct observation of magnetic relaxation in a small permalloy disk by time-resolved scanning Kerr microscopy', *Phys. Rev. Lett.*, 1997, **79**, pp. 1134–1137
2 Acremann, Y., Back, C.H., Buess, M., Portmann, O., Vaterlaus, A., Pescia, D., and Melchior, H.: 'Imaging precessional motion of the magnetization vector', *Science*, 2000, **290**, pp. 492–495
3 Hiebert, W.K., Ballentine, G.E., and Freeman, M.R.: 'Comparison of experimental and numerical micromagnetic dynamics in coherent precessional switching and modal oscillations', *Phys. Rev. B.*, 2002, **65**, pp. 140404-1–140404-4

4 Gerrits, TH., van den Berg, H.A.M., Hohlfeld, J., Bar, L., and Rasing, TH.: 'Ultrafast precessional magnetization reversal by picosecond magnetic field pulse shaping', *Nature*, 2002, **418**, pp. 509–512
5 Barman, A., Kruglyak, V.V., Hicken, R.J., Marrows, C.H., Ali, M., Hindmarch, A.T., and Hickey, B.J.: 'Characterization of spin valves fabricated on opaque substrates by optical ferromagnetic resonance', *Appl. Phys. Lett.*, 2002, **81**, pp. 1468–1470
6 Park, J.P., Eames, P., Engebretson, D.M., Berezovsky, J., and Crowell, P.A.: 'Spatially resolved dynamics of localized spin-wave modes in ferromagnetic wires', *Phys. Rev. Lett.*, 2002, **89**, pp. 277201-1–277201-4
7 Acremann, Y., Kashuba, A., Buess, M., Pescia, D., and Back, C.H.: 'Magnetic spatial non-uniformities on the picosecond timescale', *J. Magn. Magn. Mater.*, 2002, **239**, pp. 346–350
8 Barman, A., Kruglyak, V.V., Hicken, R J., Kundrotaite, A., and Rahman, M.: 'Anisotropy, damping and coherence of magnetization dynamics in a 10 μm square $Ni_{81}Fe_{19}$ element', *Appl. Phys. Lett.*, 2003, **82**, pp. 3065–3067
9 Hicken, R.J., and Wu, J.: 'Observation of ferromagnetic resonance in the time domain', *J. Appl. Phys.*, 1999, **85**, pp. 4580–4582
10 Keil, U.D., Gerritsen, H.J., Haverkort, J.E.M., and Wolter, J.H.: 'Generation of ultrashort electrical pulses with variable pulse widths', *Appl. Phys. Lett.*, 1995, **66**, pp. 1629–1631
11 Cherif, S.M., Roussigne, Y., Dugautier, C., and Moch, P.: 'Shape effect on in-plane anisotropy in magnetic dots', *J. Magn. Magn. Mater.*, 2002, **242–245**, pp. 591–593